Report no. changed (Mar 2006): SM-329-UU

SACLANTCEN MEMORANDUM
serial no: SM- 329

SACLANT UNDERSEA RESEARCH CENTRE REPORT

Water masses, sound velocity structure and circulation between the eastern Algerian Basin and the Strait of Sicily in October 1996

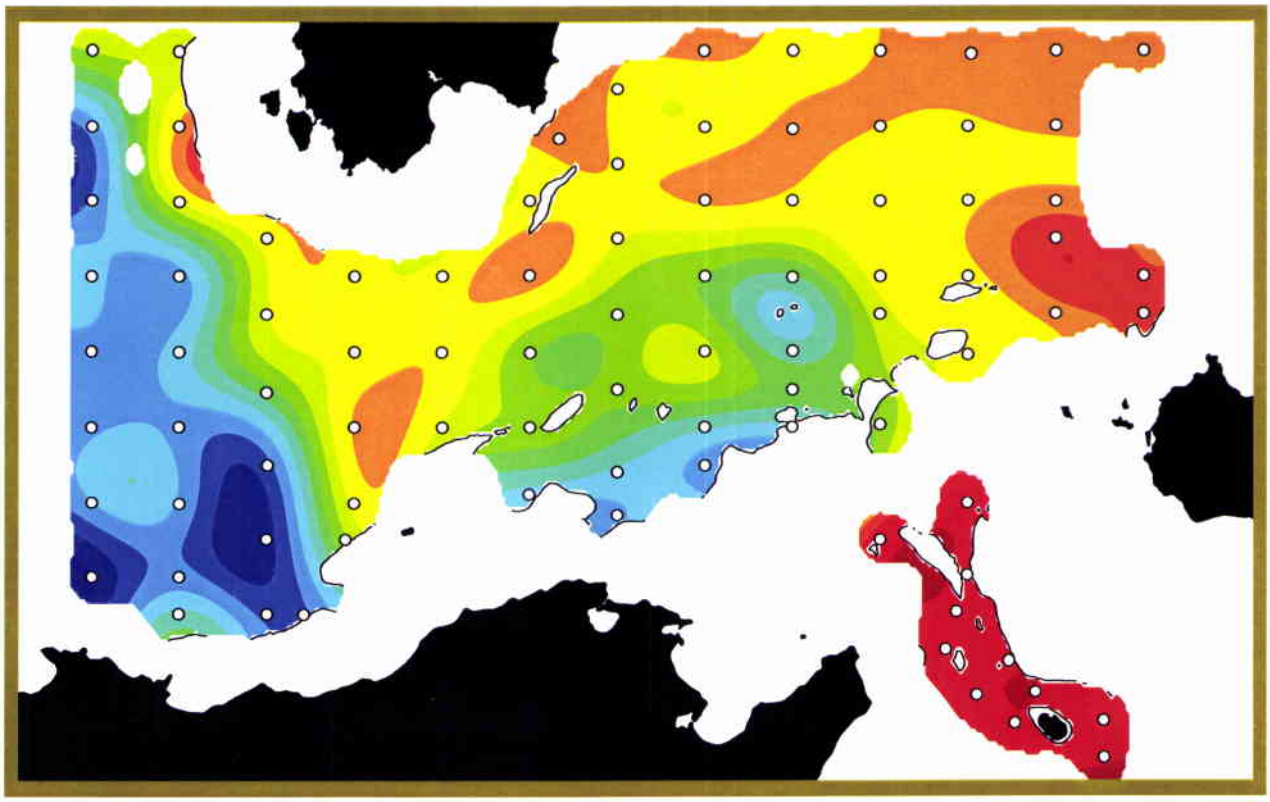

Reiner Onken and Jürgen Sellschopp

January 2002

NORTH ATLANTIC TREATY ORGANIZATION ORGANISATION DU TRAITE DE L'ATLANTIQUE NORD

Water masses, sound velocity structure and circulation between the eastern Algerian Basin and the Strait of Sicily in October 1996

Reiner Onken and Jürgen Sellschopp

The content of this document pertains to work performed under Project 01A of the SACLANTCEN Programme of Work. The document has been approved for release by The Director, SACLANTCEN.

Jan L. Spoelstra
Director

intentionally blank page

Water masses, sound velocity structure and circulation between the eastern Algerian Basin and the Strait of Sicily in October 1996

Reiner Onken and Jürgen Sellschopp

Executive Summary: The investigation is based on data collected in October 1996 between the eastern Algerian Basin and the Strait of Sicily and in the southern Tyrrhenian Sea. The major pathways of water masses are identified by the core method, and geostrophic currents and sound velocity are calculated from CTD and XCTD casts.

The sound velocity structure, which controls underwater detection conditions, is investigated in terms of the depth of the sound channel. The depth of the sound channel decreases from south to north, and is controlled by two major fronts. Typical depth changes across the fronts are 50 m over 20 km. A comparison with sound channel depth obtained from GDEM climatology reveals that in large parts of the survey area the depth was significantly greater in October 1996. This demonstrates the necessity of real time measurements.

intentionally blank page

Water masses, sound velocity structure and circulation between the eastern Algerian Basin and the Strait of Sicily in October 1996

Reiner Onken and Jürgen Sellschopp

Abstract: The investigation is based on data collected between the eastern Algerian Basin and the Strait of Sicily and in the southern Tyrrhenian Sea. The major pathways of water masses are identified by the core method and geostrophic currents are derived from the objectively analyzed density field.

Between the Sardinia Channel and the Strait of Sicily, the large-scale circulation of Modified Atlantic Water (MAW) and Winter Intermediate Water (WIW) is found to be cyclonic. Inflow into the gyre occurs via the Sardinia Channel by means of a boundary current attached to the Algerian coast, and from the northern Tyrrhenian. The outflow is accomplished via the Strait of Sicily and to the Tyrrhenian. The Levantine Intermediate Water (LIW) flow resembles that of MAW/WIW in the southern Tyrrhenian, but it is opposed in the Strait of Sicily and off Tunisia. Outflow to the Algerian Basin occurs south of Sardinia. In the eastern Algerian Basin the flow direction of all water masses is eastward close to the Algerian shelf. Farther offshore, MAW flows mainly southwest whereas the LIW is opposed to that supporting northward transport along the Sardinian shelf. The large-scale flow of all water masses is perturbed by mesoscale eddies. The impact of topographic obstacles is investigated.

Keywords: Mediterranean ◦ Modified Atlantic Water ◦ Winter Intermediate Water ◦ Levantine Intermediate Water

Contents

List of Figures

List of Tables

intentionally blank page

1

Introduction

In October 1996, a hydrographic survey was conducted by the NATO Research Vessel *Alliance*. The survey area (Fig. 1) is centred approximately between Sardinia, Sicily and Tunisia, and extends into the western Algerian Basin, the southern Tyrrhenian and the western part of the Strait of Sicily. The campaign was motivated by the fact that this area is one of the less well understood of the Mediterranean, although it is a crossroads for the water masses in the Western Mediterranean, namely Modified Atlantic Water (MAW), Winter Intermediate Water (WIW), Levantine Intermediate Water (LIW), and the deep water masses. Because the majority of the measurements were limited to depths shallower than about 1000 m, the objective of this study is to investigate the distribution of MAW, WIW, and LIW and to provide a consistent circulation pattern.

MAW originates from the inflow of Atlantic water through the Strait of Gibraltar. It is the surface water of the Mediterranean and occupies the 100–200 m depth range. Evaporation and mixing increase progressively the salinity along its path; however,

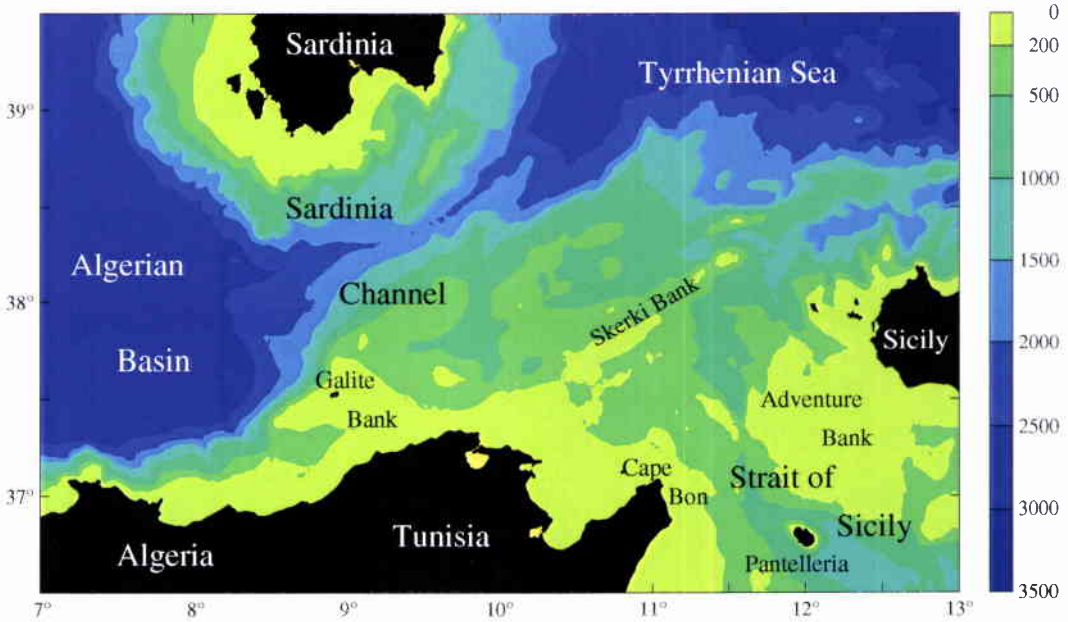

Figure 1 *Bathymetry [m] and geographic names of the survey area.*

because evaporation affects mainly the mixed-layer salinity, MAW can be traced by a subsurface salinity minimum. The MAW inflow into the survey area is from the west by means of the Algerian Current. According to older literature, the flow separates at the entrance of the Sardinia Channel into a northward branch along Sardinian west coast and a southern one heading east towards the Strait of Sicily. More recent observations and models suggest northward flow along the west coast of Sardinia only in winter. The major part of MAW leaves the survey area via the Strait of Sicily towards the Eastern Mediterranean (Bethoux, 1980). The rest proceeds into the Tyrrhenian, and partly recirculates cyclonically to the Sardinia Channel. For further information on the circulation in the Tyrrhenian, the reader is referred to the review of Astraldi and Gasparini (1994).

WIW is formed in the Western Mediterranean by surface cooling of MAW during winter in the Ligurian Sea and off the Catalan coast (Lacombe and Tchernia, 1960; Salat and Font, 1987). After restratification of the near surface layers, WIW becomes insulated and can be traced by means of a temperature minimum between about 100 and 200 m depth. Up to now, the circulation of WIW has been investigated only in the Algerian Basin, and there is evidence that it follows approximately the same flow paths as the overlying MAW (see also Fig. 1 of Millot, 1999).

LIW originates from convection in the Eastern Mediterranean, and can be identified by means of a salinity maximum at intermediate depths. From the source region, LIW spreads westward and spills over the sills of the Strait of Sicily. The further fate is controversial; Wüst (1961) suggested one part to turn north around Sicily, and a westward branch to continue straight ahead to the Sardinia Channel. Evidence for this was also found by Garzoli and Maillard (1979) and is reproduced by some recent numerical models. By contrast, the latter branch was not verified by Ovchinnikov (1966). According to his calculations, the LIW proceeds to the southern Tyrrhenian and then bifurcates into one part joining the basin-scale cyclonic gyre, and another one performing a shorther cyclonic loop. Both reunite in the southwestern Tyrrhenian and leave the basin via a concentrated flow around the southern tip of Sardinia. Later, elements of essentially the same pattern were also identified by other authors.

The above review has shown that there exists detailed knowledge of the circulation in the survey area, but many findings are contradictory. The obvious reason for this is that the knowledge was accumulated from many surveys, none of which was synoptic with respect to the entire region. A possible way out of this situation could be to take a mean over all observations and create a "climatology", however, this would smooth or even delete the majority of mesoscale features and pretend a situation which never exists. Therefore, the major objective of this paper is to present a synoptic picture of the distribution and circulation of water masses.

2

Data and methods

The oceanographic survey covered the period 19–31 October 1996. The data discussed here consists of casts from CTD (Conductivity-Temperature-Depth), XCTD (Expendable CTD), and XBT (Expendable Bathythermograph). In addition, we shall refer to currents measured by shipborne ADCP (Acoustic Doppler Current Profiler), and AVHRR (Advanced Very High-Resolution Radiometer) satellite data of sea surface temperature. The casts were arranged mostly on parallel meridional tracks spaced $\approx$ 36.5 km apart (Fig. 2), the nominal along-track spacing between individual casts was $\approx$ 15.7 km. In deep water, the majority of CTD casts was limited to about 1000-m depth, the maximum vertical extent of XCTDs was around 1000 m, that of XBTs close to 750 m.

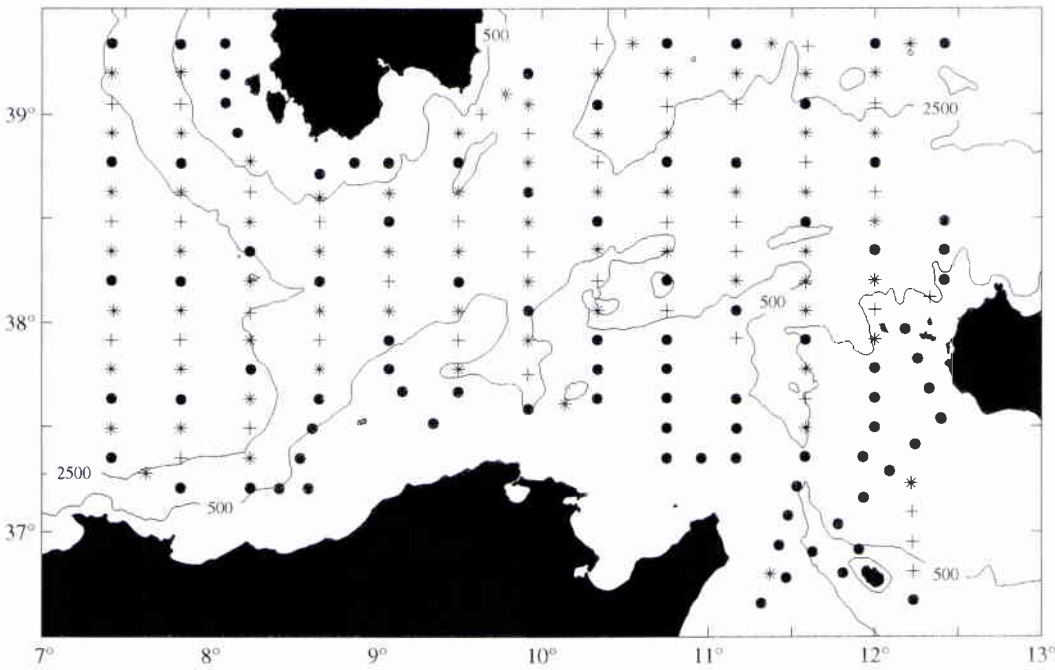

Figure 2 *Positions of CTD(•), XCTD(+), and XBT (∗) measurements. Lines indicate water the 500-m and 2500-m depth contours.*

Objective analysis (Carter and Robinson, 1987) is applied throughout, whenever any scalar variable is to be displayed on horizontal or quasi-horizontal surfaces. The employed correlation scale of 40 km is a compromise between the desire to resolve mesocale features on the one hand and taking account of the track spacing on the other hand. The observational error ϵ is defined to be 10% of the standard deviation of the observations.

3

MAW

In order to visualize the horizontal distribution of MAW, CTD and XCTD profiles were scanned for a subsurface salinity minimum and subsequently, $S(S_{min})$ and $p(S_{min})$, the salinity and the pressure of the minimum, were objectively analysed. Over the major part of survey area, $p(S_{min})$ lies between about 30 and 70 dbar (Fig. 3, bottom). Larger values of up to 100 dbar and more are found in a $\approx$ 30 km wide stripe extending along the Algerian/Tunisian coast up to Cape Bon. Provided that low $S(S_{min})$ values correspond to "young" MAW, Fig. 3 reveals that MAW enters the survey area from the west close to the Algerian coast. At about 11°E, the low salinity vein splits in two branches. One turns south around Cape Bon and the other is directed northeast towards the Tyrrhenian. Here, according to the shape of the the 37.7 and 37.8 isohalines, there is indication that MAW partially recirculates to the west. The rather high $S(S_{min})$ values south and east of Sardinia exceeding 37.7 suggest this MAW to be rather old, it probably performed a basin-scale cyclonic loop in the Tyrrhenian and returns to the Sardinia Channel. Other patches of high $S(S_{min})$ are located between Sicily and Pantelleria.

As the core method allows to make only limited conclusions on the predominant pathways of water masses, the geostrophic currents averaged over the MAW vertical range were calculated from the objectively analyzed density field. WIW is the water mass next to MAW, hence the lower MAW boundary was selected as $0.5 \cdot [p(S_{min}) + p(T_{min})]$, where $p(T_{min})$ is the pressure of the WIW temperature minimum (see below). Although the geostrophic velocity (Fig. 4) is perturbed by mesoscale eddies, it is possible to identify larger-scale flow paths. The dominant feature is an intense boundary current heading eastward along the Algerian/Tunisian coast and then turning south into the Strait of Sicily. Maximum speeds are reaching almost 60 cm s^{-1} east of Cape Bon. West of the Sardina Channel, this current apparently is the eastward continuation of the Algerian Current, but in the Channel, it is in addition fed by another flow coming from west of Sardinia. At about 11°E, part of the current splits off generating a branch directed east. When approaching Sicily, this branch separates again into southward flow and a northern branch towards the eastern Tyrrhenian. Part of the latter recirculates to the west forming a cell of about 100-km size between Sicily and Sardinia. At its northern flank, this cell is also fed by MAW coming from the central Tyrrhenian. In the Sardinia Channel, the flow is eastward just off the Sardinian coast and a band of westward flow is located about 30′ farther south. It appears that this westward flow

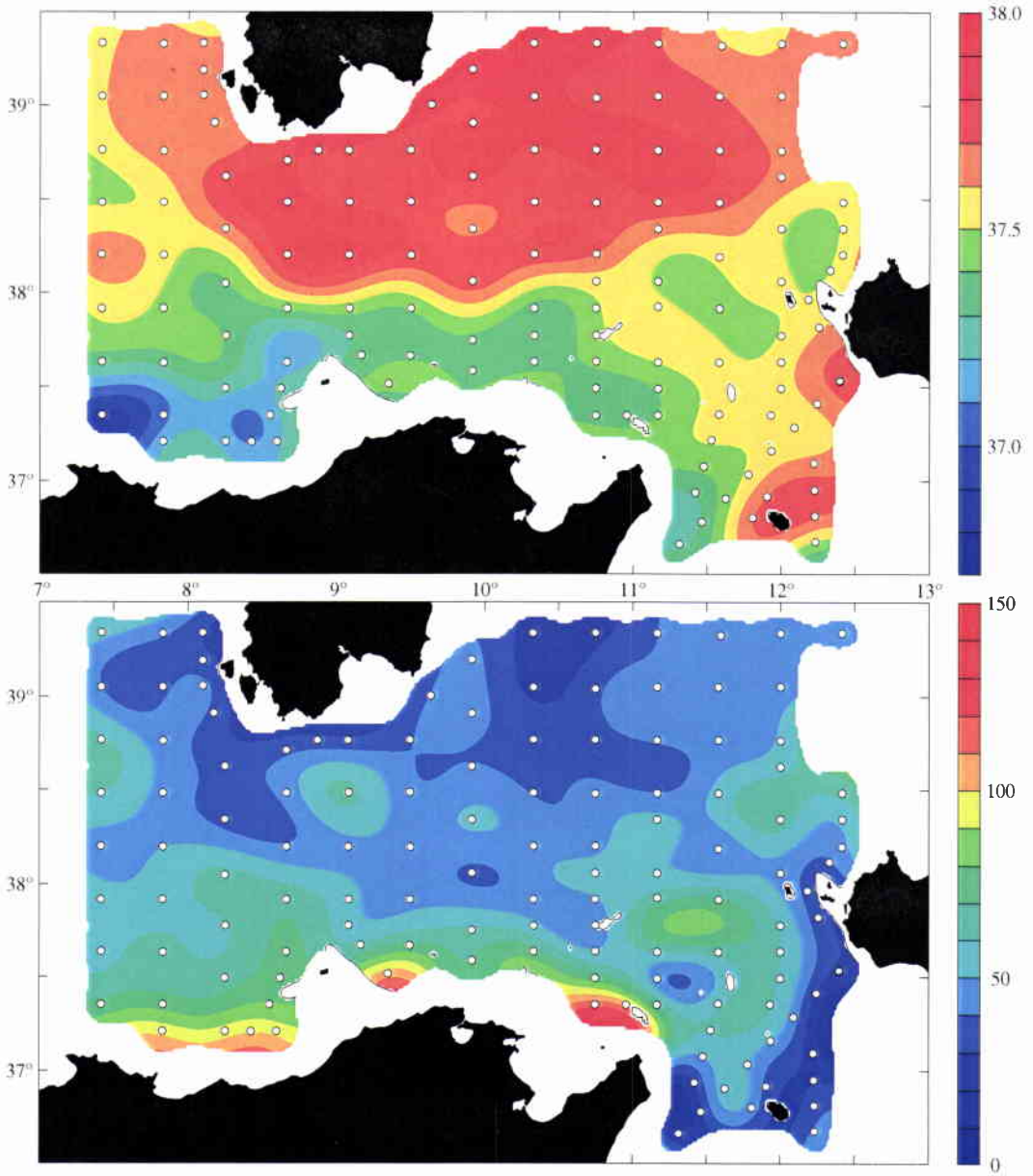

Figure 3 *Objectively analysed salinity $S(S_{min})$ (top) and pressure $p(S_{min})$ [dbar] (bottom) of the MAW salinity minimum. White dots indicate stations where a subsurface salinity minimum was found. Black solid lines denote the intersection of the $p(S_{min})$ surface with the bathymetry H. Areas where the root mean square error of the analysed fields is greater than 2ϵ or $p(S_{min}) > H$ are left white.*

recirculates to the east by means of a cyclone/anticyclone pair. Hence, there is no visible westward return flow across the Sardinia Channel. Two outstanding features which have not yet been addressed, are the anticyclonic eddies located over Adventure Bank and east of Sardinia, to be denoted as the Adventure Bank anticyclone and the Sardinia anticyclone. The latter appears to entrain MAW from the cyclonic recirculation mentioned before and the major part of MAW flowing eastward off the Sardinian south coast. The Adventure Bank anticyclone is apparently fed by the eastward branch immediately after flow splitting at 11°E. At its southwestern flank, this eddy contributes to the southward boundary current off Tunisia.

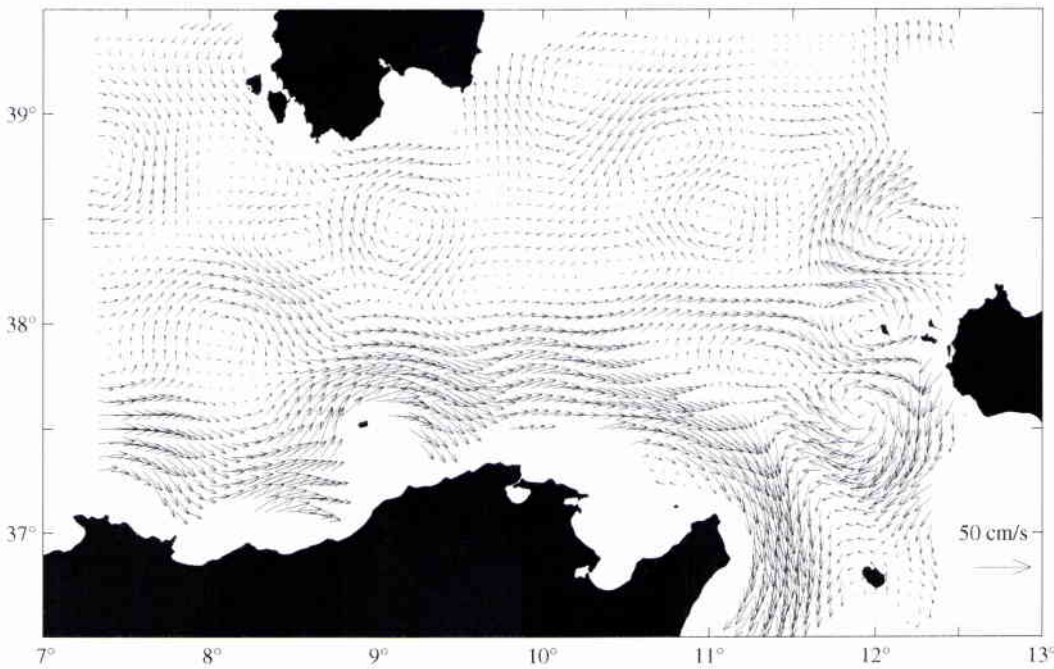

Figure 4 *MAW mean geostrophic velocity assuming a level of no motion at 1000 dbar. For definition of the MAW layer see text. Only every 4th vector was plotted.*

For validation of the geostrophic flow pattern, we have provided ADCP measurements of the near surface velocity field. Without going to much into detail, Fig. 5 resembles Fig. 4, except for the pattern west of Sardinia and the anticyclonic meander of the Algerian Current at about (8°W, 38°N), which is not reflected by the ADCP measurements. Probably, these differences are due to the different ranges of vertical averaging (fixed range for ADCP, variable lower boundary for the geostrophic currents). In addition, the ADCP currents are generally stronger than the geostrophic, which is obviously caused by the smoothing of the objective analysis of the density field.

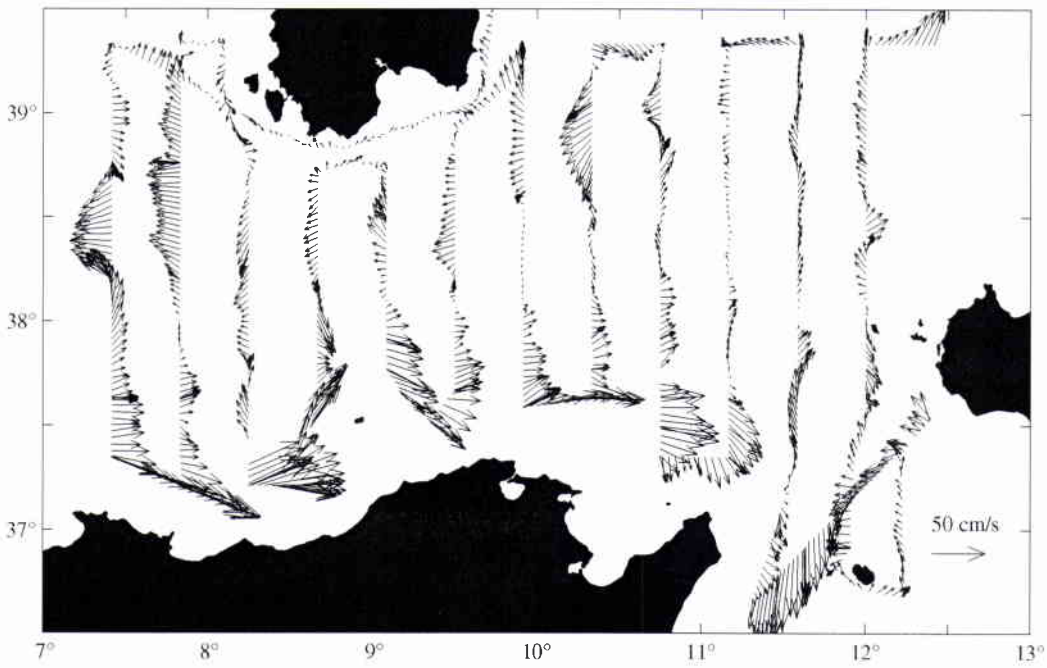

Figure 5 *Directly measured currents from shipborne ADCP, averaged over the vertical range 18–98 m. Each vector represents a 10-minutes ensemble average.*

Further validation may be obtained from a satellite image of sea surface temperature (Fig. 6). The eyecatching feature is the northwest/southeast oriented front which extends over the entire survey area, separating warm water (temperature $> 18°$) in the south from colder water in the north. The position of the front closely resembles that of the 37.52 isohaline of Fig. 3, hence the front apparently forms the boundary between new MAW from the Algerian Basin and recirculated MAW. A warm tongue directed towards the Tyrrhenian clearly indicates the flow separation at 11°E. The Adventure Bank anticyclone appears as a warm patch, and the link between the eddy and the MAW flow around Cape Bon is visible by means of a frontal meander. A warm filament centred at about (10°E, 39°N) matches the azimuthal flow of the Sardinia anticyclone.

The geostrophic circulation has revealed several features which were expected from previous knowledge; other features appear to be unfamiliar and deserve to be discussed. This is for example, the northern branch of the inflow into the Sardinia Channel coming from west of Sardinia. Such a current contradicts Lacombe and Tchernia (1972), and Ovchinnikov (1966), but it agrees rather well with the observations of Garzoli and Maillard (1979) and the models of Zavatarelli and Mellor (1995) and Roussenov et al. (1995). They show that in winter, northward flow west of Sardinia is due to cyclonic surface circulation between Sardinia and the Balearic Islands, while in summer, it is anticyclonic contributing to a secondary in-

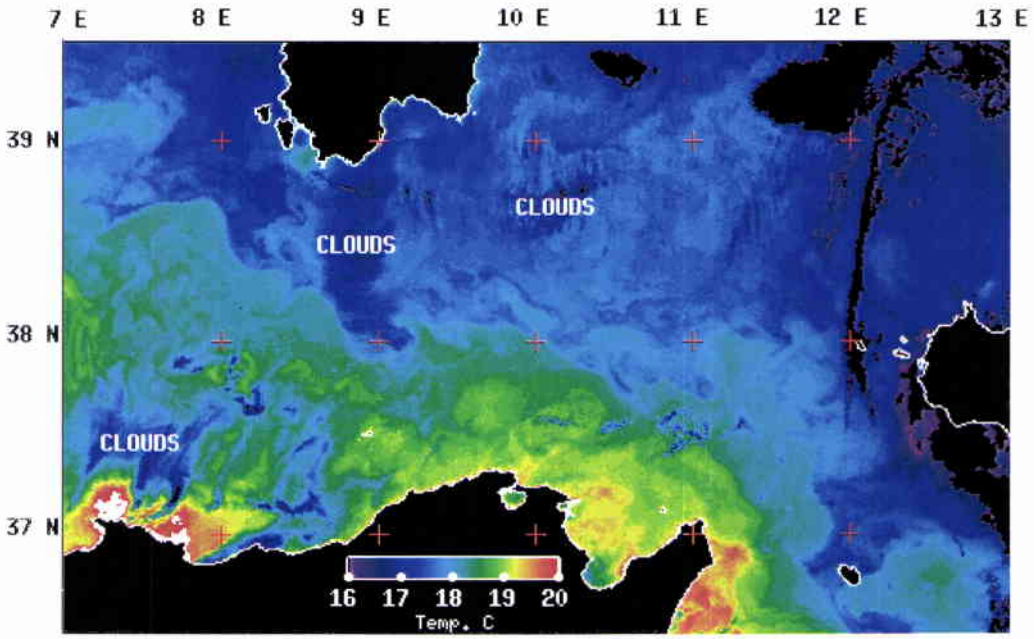

Figure 6 *AVHRR infrared (Channel 4) image of sea surface temperature, taken by the TIROS-N NOAA14 satellite on 29 October 1996 at 12:56 UTC. Temperatures outside the range 16 – 20° C are black and white, respectively.*

flow into the Sardinia Channel. This branch is also visible in the model of Herbaut et al. (1998). Although our survey was in fall, it obviously reproduces this feature. Closely related to that is the direction of flow in the Channel. By contrast to the climatological studies of Lacombe and Tchernia (1960, 1972) and Ovchinnikov (1966) and the synoptic survey of Bouzinac et al. (1999), there is no indication for a westward vein close to the Sardinian coast. The flow direction resembles more the results of Garzoli and Maillard (1979) and Perkins and Pistek (1990). In the latter studies, the flow along the Algerian coast was westward, probably forced by a large anticyclonic eddy. Such eddy was not found in the present survey, however, the anticyclonic meander of the Algerian Current at 8°E may be interpreted as a leftover of such feature.

The meridional extent of the recirculation path in the Tyrrhenian varies seasonally (Krivosheya and Ovchinnikov, 1973; Krivosheya, 1983; Pierini and Simioli, 1998). In winter, the surface circulation exhibits a basin-scale cyclonic gyre, whereas in summer the major recirculation is confined to south of about 40°N. In satellite images, this becomes visible by a strong temperature front between Sardinia and Sicily (Marullo et al., 1994). In the present survey, the recirculation occurs via two paths; a well defined tight recirculation cell is confined to south of 39°N, and there is ev-

idence for larger scale recirculation extending farther north. Hence, the October survey exhibits elements both of the summer and winter circulation. This transitional state is supported by Fig. 6, which does not show any strong temperature front in the southern Tyrrhenian.

Both the Sardinia anticyclone and the Adventure Bank anticyclone are not verified by any climatological study, but there is indication from a few synoptic observations that they are recurrent features. The first was already identified by Krivosheya and Ovchinnikov (1973) as an "intense and stable" eddy, and a vein of MAW flow to the Tyrrhenian near the coast of Sardinia was observed by Garzoli and Maillard (1979). The Adventure Bank anticyclone was never mentioned before, but in conjunction with previous knowledge we conjecture that it is recurrent during summer. According to climatological observational studies and models, the flow in the Strait of Sicily occurs by means of a wide current extending over the entire width of the Strait, with weak evidence of stronger flow on the Tunisian side. By synoptic observations, this pattern is partly confirmed, but only for winter. More often in summer, the flow was found to split into several branches; part of the outflow still hugs the Tunisian coast, but another significant fraction apparantly occurs close to Sicily (Garzoli and Maillard, 1979; Manzella et al., 1988; Astraldi et al., 1996; Robinson et al., 1999). It is suggested that this vein is forced by the eastward branch of MAW after the flow splitting at 11°E. When impinging on the west coast of Sicily, part of this becomes deflected to the south, thus stimulating anticyclonic circulation in this area. Furthermore, from Robinson et al. (1999) and Onken and Sellschopp (1998) it is known that a recurrent feature of the summer circulation is the Adventure Bank vortex, a cyclone which occupies the eastern slope of Adventure Bank. Hence, we conjecture that the enhanced southward flow part of the Adventure Bank anticyclone is partly forced by the Adventure Bank vortex.

Due to the smoothing of objective analysis, there is no evidence from Fig. 4 that the major topographic obstacles, Skerki Bank and Galite Bank, have any impact on the MAW flow path. By contrast, ADCP measurements clearly reveal a seaward deflection of the near surface flow by Galite Bank, but no deflection occurs over Skerki Bank. Probably, the depth and the shape of the topographic features are the reasons for this different behavior. The horizontal extent and orientation of both obstacles is similar, but the region where the water depth is less than 100 m forms a connex area with Galite Bank, while the shallows of Skerki Bank are scattered. Hence, the dynamical impact of Galite Bank is similar to that of a seamount – it has to be circumvented anticyclonically. Skerki Bank is acting more like a seamount chain, where the fluid can pass through the gaps. This is in agreement with the distribution of the MAW salinity minimum in Fig. 3 (top), where the low salinity tongue is deflected north by Galite Bank, but is not hindered by Skerki Bank.

4
WIW

In order to explore the distribution of WIW, all casts were scanned for a temperature minimum T_{min}. The objectively analyzed distribution of $T(T_{min})$ and $p(T_{min})$ (the temperature and pressure of the minimum) in Fig. 7 reveal $T(T_{min})$ values $\leq 13.5°C$ southwest of a front extending from the northwest corner of the survey area to Galite Bank. Centered at about 38°N, a cold tongue extends east as far as $\approx 12°E$. Opposed to that, a warm tongue is directed west north of 38°N. Provided that $T(T_{min})$ increases along the flow path, WIW obviously enters the survey region from the west close to the Algerian coast. A secondary region of low $T(T_{min})$ is located east of Sardinia. Over the major part of the survey area, $p(T_{min})$ lies between 100 and 200 dbar. South of the front mentioned above and along the Algerian/Tunisian shelf slope, larger values of up to 280 dbar are attained. Another region of large $p(T_{min})$ corresponds to the position of the low $T(T_{min})$ value east of Sardinia. No T_{min} was identified east of Cape Bon. Hence, WIW apparently does not enter the Strait of Sicily, or T_{min} is eroded completely by mixing. The latter is supported by the T/S diagram (Fig. 12), where traces of WIW are identified on the Tunisian side of the Strait of Sicily.

For the calculation of geostrophic flow (Fig. 8), the upper boundary is identical with the lower MAW boundary defined above, and the lower boundary was defined as $0.5 \cdot [p(T_{min}) + p(S_{max})]$, where $p(S_{max})$ is the pressure of the LIW salinity maximum (see below). Apart from the fact being weaker, the flow pattern exhibits many similarities with that of MAW, but there are significant differences: For MAW, the flow west of Sardinia is mainly south, whereas the corresponding WIW flows in different directions. Another difference is the circulation over Skerki Bank. The Bank did not seem to be a major obstacle for MAW, WIW however, is blocked and circumvents the Bank anticyclonically.

In concert with Sammari et al. (1999), this study is the first referring explicitly to the distribution and circulation of WIW within and east of the Sardinia Channel. However, by re-interpretation of previous publications, there is evidence that WIW is permanently present in this area. In the Sardinia Channel, WIW was encountered by Perkins and Pistek (1990, their Fig. 4) everywhere. Essentially the same situation was described by Bouzinac et al. (1999), but they identified two veins on the Algerian and Sardinian side of the Channel. Further evidence is gained from Katz (1972), who clearly found WIW between Sicily and Sardinia and in the southern Tyrrhenian (see

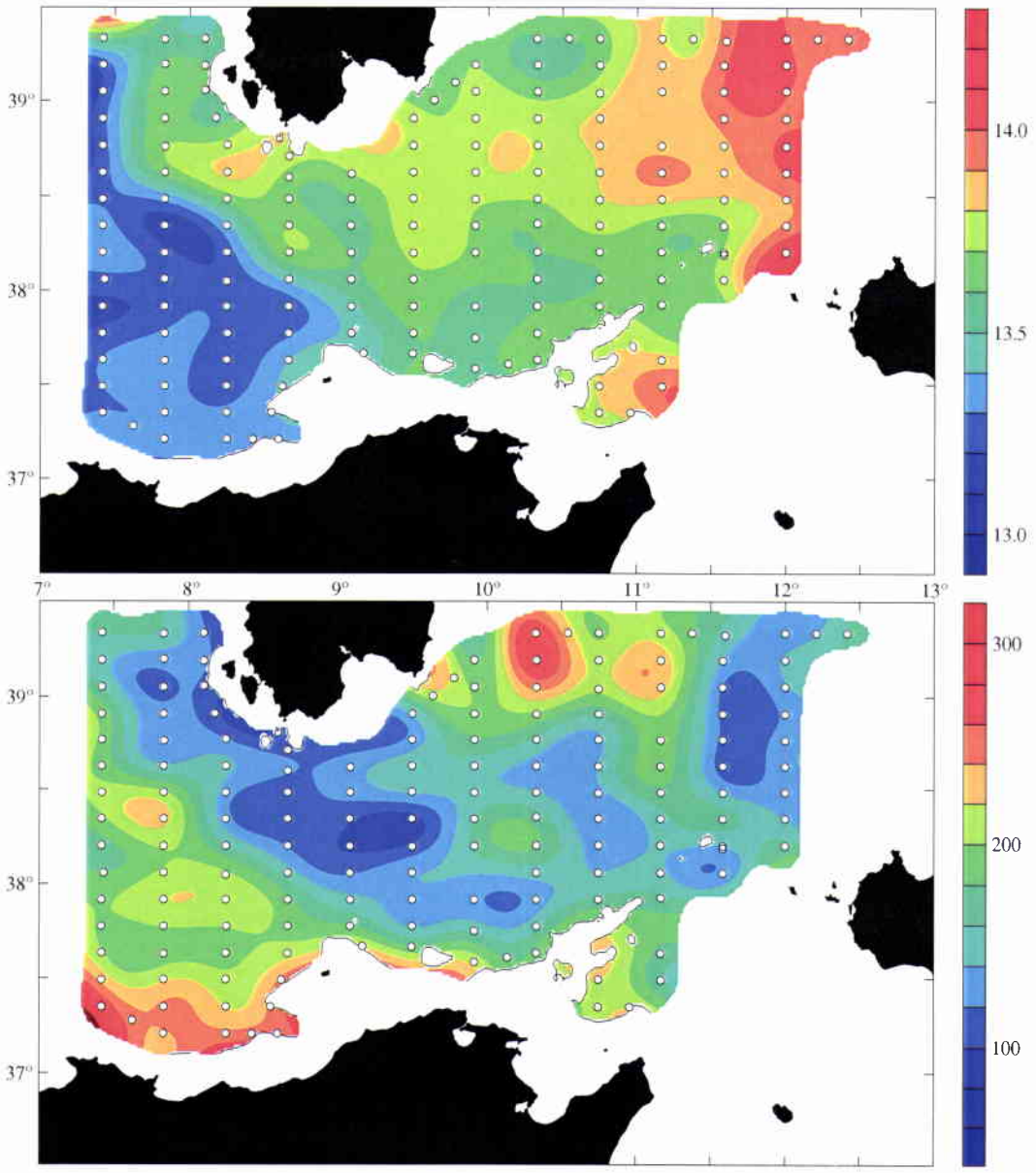

Figure 7 *Objectively analysed temperature $T(T_{min})$ (top) and pressure $p(T_{min})$ [dbar] (bottom) of the WIW temperature minimum. White dots indicate stations where a subsurface temperature minimum was found. Black solid lines denote the intersection of the $p(T_{min})$ surface with the bathymetry H. Areas where the root mean square error of the analysed fields is greater than 2ϵ or $p(T_{min}) > H$ are left white.*

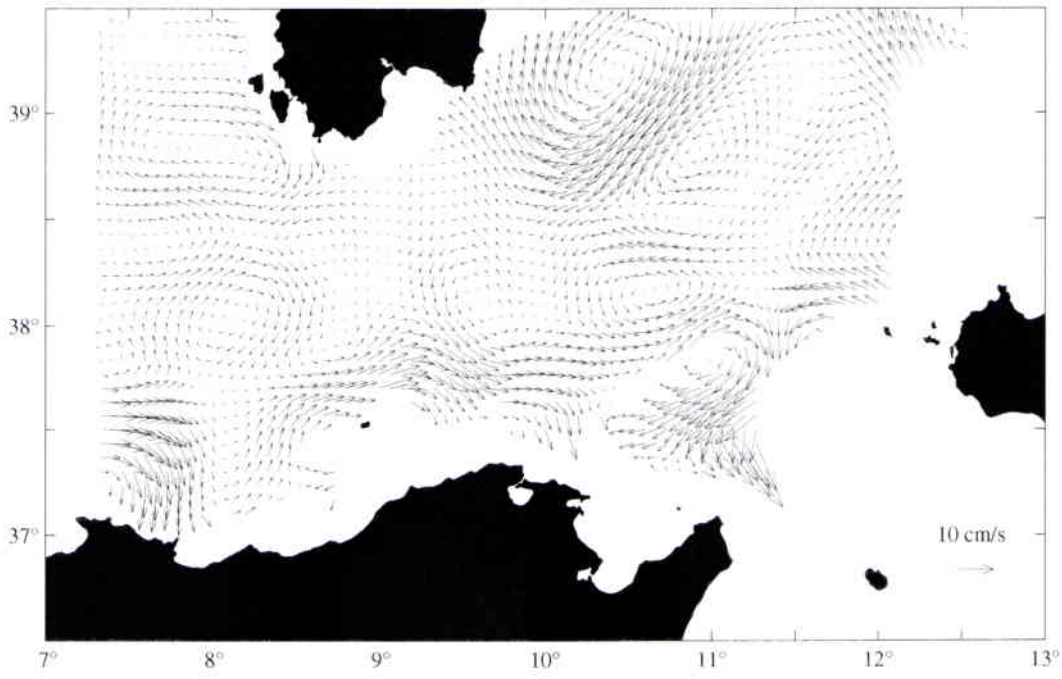

Figure 8 *WIW mean geostrophic velocity assuming a level of no motion at 1000 dbar. For definition of the WIW layer see text. Only every 4th vector was plotted.*

his Fig. 11). All CTD sections across the Sardinia Channel described by Sammari et al. (1999) show T_{min} at about 170 m depth; similar values were encountered by Bouzinac et al. (1999). On our survey, T_{min} lies shallower by several tens of metres, and Perkins and Pistek (1990) even found it between 200 and 400 m. In addition, $T(T_{min})$ varies among the surveys by some tenths of a degree. Hence, the WIW location and characteristics seem to be variable, but we cannot decide yet whether this is due to interannual variability of WIW formation, seasonal variability, or simply a dynamical response to mesocale processes. Alternatively, it has to be taken into account that WIW may be produced locally (cf. Hopkins, 1988). Support is provided by Krivosheya (1983) suggesting another formation site in the northern Tyrrhenian, and from climatological data bases (cf. Mediterranean Oceanic Data Base, available at Internet site http://modb.oce.ulg.ac.be). The latter reveals that in the western Tyrrhenian, the surface temperature may drop to 13°C in winter, which is similar to $T(T_{min})$ in Fig. 7.

In the western part of the Strait of Sicily, water with pronounced WIW characteristics was identified before by Frassetto (1972), Molcard (1972), Shonting and Nacini (1972), Garzoli and Maillard (1979), and Astraldi et al. (1996), but only in winter and spring and never in summer or autumn. As also in our October survey we merely detected remnants of WIW in the Strait, we hypothesize that the circulation

undergoes a seasonal cycle; WIW enters the Strait in winter/spring when the eastward MAW flow is strongest (Manzella, 1994) and is subsequently mixed in summer and autumn loosing its properties.

5
LIW

LIW is characterized by an absolute maximum of salinity at intermediate depth. The analyzed distribution of $S(S_{max})$ and $p(S_{max})$ (the salinity and pressure of the maximum) are shown in Fig. 9. Provided that $S(S_{max})$ decreases along the main path, Fig. 9 suggests LIW to enter the survey region via the Strait of Sicily, where the highest $S(S_{max})$ values close to 38.8 are found near Pantelleria. Towards northwest, $S(S_{max})$ decreases rapidly by about 0.1 when approaching Skerki Bank indicating strong vertical mixing. Further evidence for strong mixing is gained from the fact that there is no intermediate S_{max} between the exit of the Strait of Sicily and the Tyrrhenian. From the eastern Tyrrhenian, a high salinity tongue $38.66 \leq S(S_{max}) \leq 38.72$ is directed west towards Sardinia. A flow splitting occurs obviously in the Sardinia Channel, where one high salinity tongue is attached to the west Sardinian shelf and another extends south towards Galite Bank. Hence, the large scale circulation in the Sardinia/Tunisia/Sicily region seems to be cyclonic. Between Galite Bank and Skerki Bank, $S(S_{max})$ lies below 38.66, the lowest values of < 38.54 being found close the Tunisian shelf. West of the Sardinia Channel, a strong front extends from Galite Bank to the northwest corner of the survey area, separating old LIW in the west from younger in the east. The $p(S_{max})$ distribution is rather patchy. Low values between 200 and 300 dbar are encountered in the Strait of Sicily and between Galite Bank and Skerki Bank. Values between 300 and 600 dbar are attained in the southern Tyrrhenian and west of 9°E, while the absolute maximum exceeding 600 dbar is attained northwest off Sicily, supporting the finding of Sparnocchia et al. (1999) that at least part of the LIW cascades to great depth in the Tyrrhenian Sea.

The geostrophic velocity, averaged between the lower boundary of WIW and 1000 dbar (Fig. 10), exhibits maximum speeds of close to 10 cm s^{-1} in the Strait of Sicily north of Cape Bon. East of the Cape, the velocity is westward and the vectors are approximately parallel to the bathymetry contours. Between Skerki Bank and Adventure Bank, the flow direction is mainly west/southwest. A northward component is only found close to Adventure Bank. A flow separation occurs at about (12°E, 38.5°N): one branch goes north and appears to perform a large-scale cyclonic loop in the southern Tyrrhenian; the other branch circumvents Skerki Bank and proceeds west. A further separation occurs southeast of Sardinia. The northern fraction of LIW recirculating from the Tyrrhenian is entrained in the Sardinia anticyclone, the southern part is directed southwest to the Tunisian coast, and the central fraction

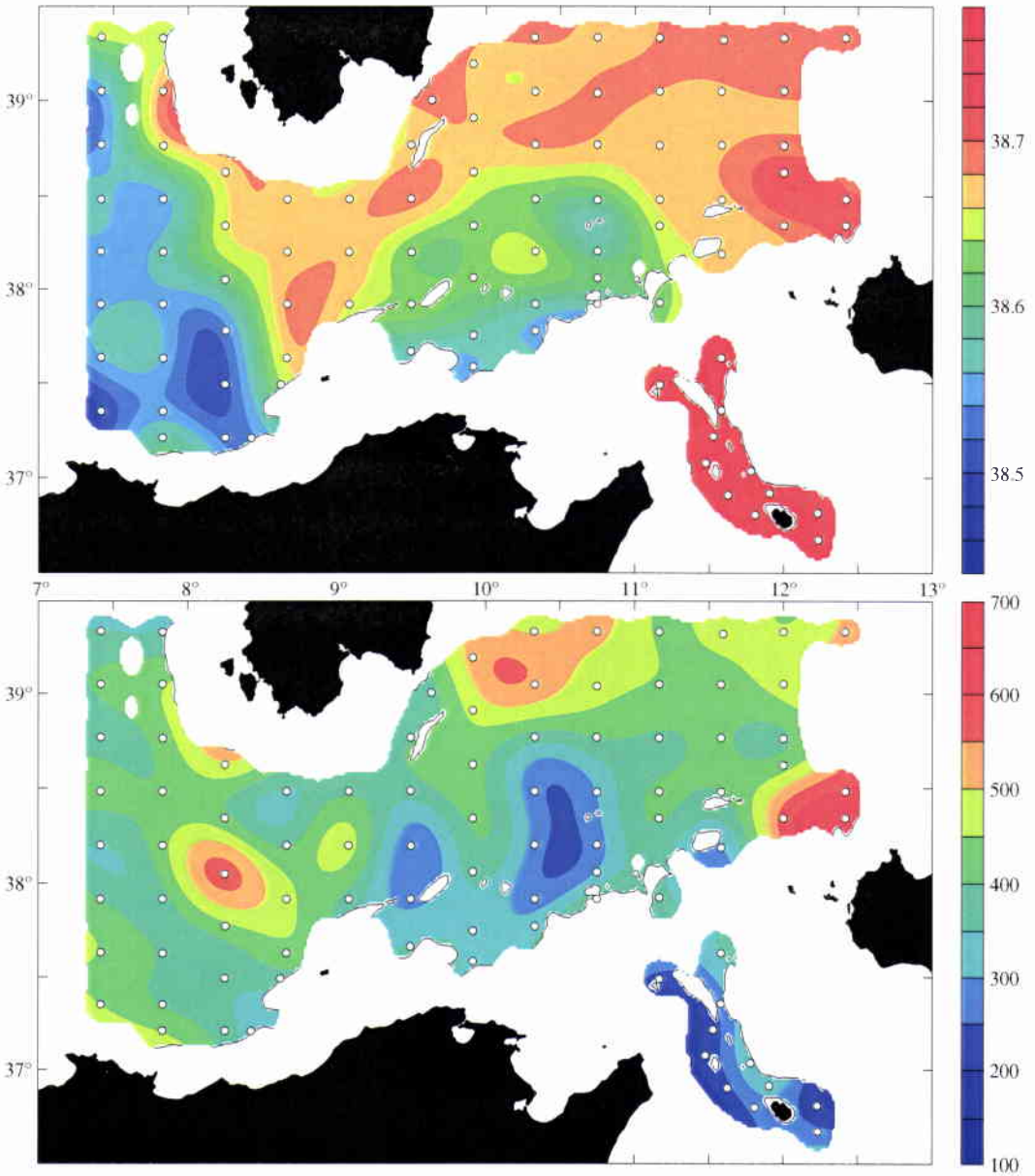

Figure 9 *Objectively analysed salinity $S(S_{max})$ (top) and pressure $p(S_{max})$ [dbar] (bottom) of the LIW salinity maximum. White dots indicate stations where a subsurface salinity maximum was found. Black solid lines denote the intersection of the $p(S_{max})$ surface with the bathymetry H. Areas where the root mean square error of the analysed fields is greater than 2ϵ or $p(S_{max}) > H$ are left white.*

proceeds west into the Sardinia Channel and circumvents Sardinia anticyclonically. In the west, the major inflow into the survey region occurs at about 37°30′ N. One fraction of that is running towards the Algerian shelf, and the other recirculates cyclonically and joins the anticyclonic flow around Sardinia.

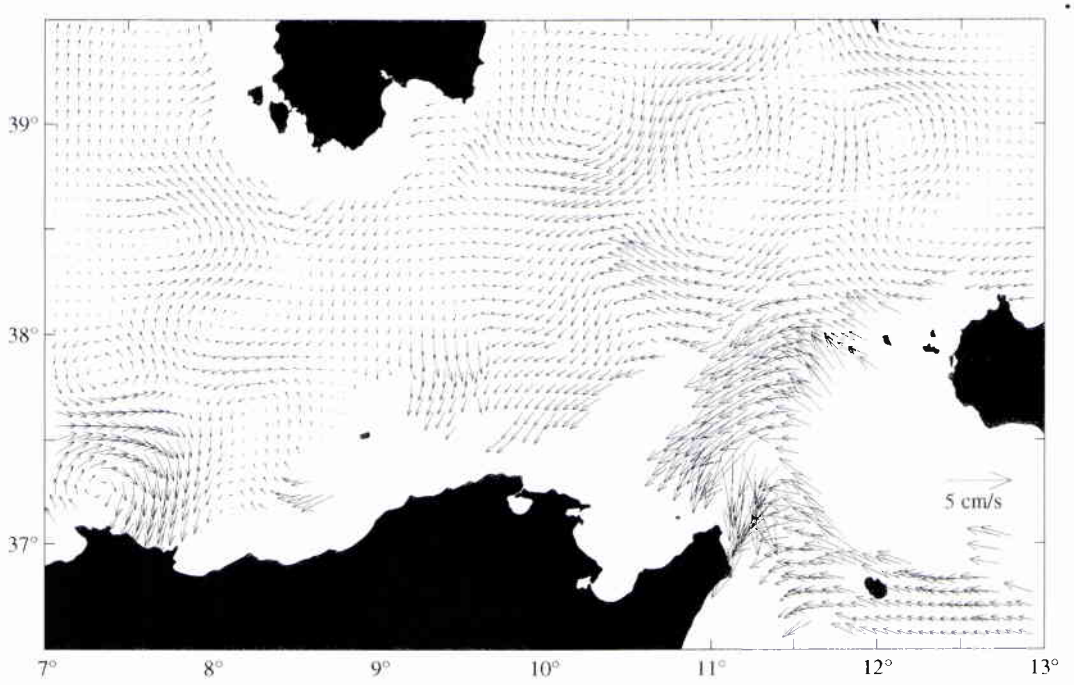

Figure 10 *LIW mean geostrophic velocity assuming a level of no motion at 1000 dbar. For definition of the LIW layer see text. Only every 4th vector was plotted.*

All along the Algerian/Tunisian shelf and on the western side of Adventure Bank, the flow exhibits a component normal to bathymetry contours. It has been verified that this unrealistic behaviour is neither due to selection of a wrong level of no motion, nor to vertical averaging. Hence, we speculate that there are either narrow along-shelf geostrophic boundary currents, which are not properly resolved by the measurements, or the boundary currents are strongly affected by ageostrophic effects, i.e. friction. It was attempted to validate also the LIW geostrophic currents by ADCP measurements, although the data quality was already very low in the respective depth range. Nevertheless, if one disregards the small-scale noisy features and makes only a qualitative comparison, Fig. 11 contains a number of consistent (i.e. visible on different ship tracks) patterns, which approximately match the geostrophic currents. This is the westward flow band in the southern Tyrrhenian, the Sardinia anticyclone, the flow around Sardinia, and the tendency of westward flow between Skerki Bank and Galite Bank. It is remarkable that also the ADCP currents do not show a continuous flow between Skerki Bank and Adventure Bank to the Tyrrhenian. Hence, there are good reasons to trust the geostrophic calculations.

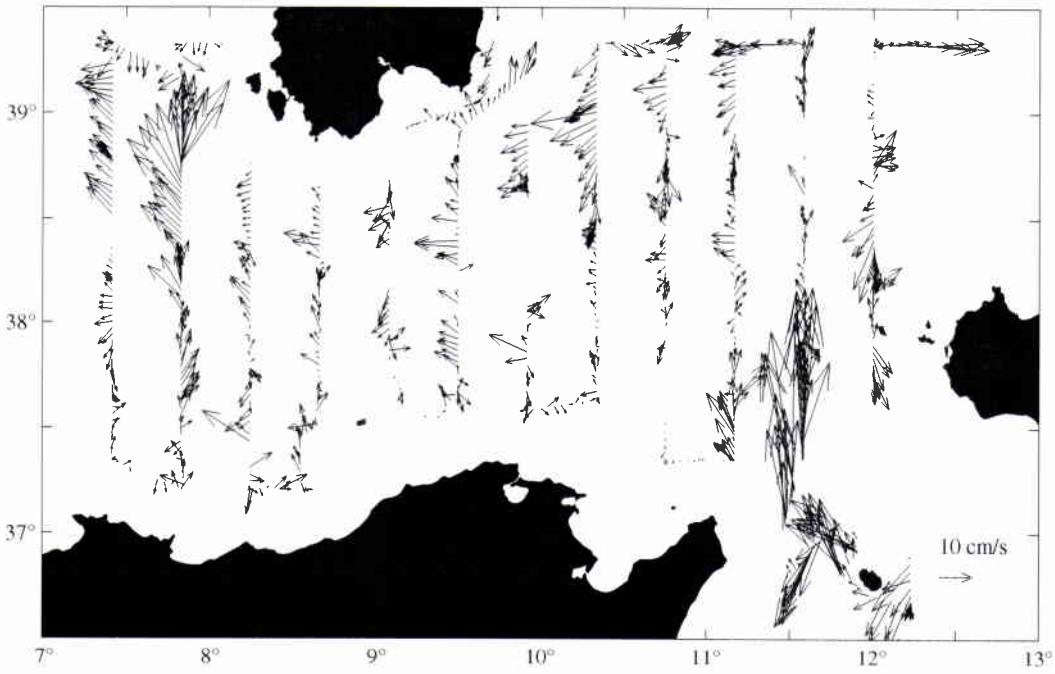

Figure 11 *Directly measured currents from shipborne ADCP, averaged over the vertical range 202–450 m representing LIW. Each vector is a 10-minutes ensemble average.*

There is evidence for a direct vein of LIW extending west from the Strait of Sicily, but this vein is only partly manifested in the $S(S_{max})$ distribution. Otherwise, the flow pattern resembles more the findings of Ovchinnikov (1966), Krivosheya and Ovchinnikov (1973), Krivosheya (1983), Hopkins (1988), and Manzella et al. (1988). It is suggested that a direct vein may be generated only under the influence of special conditions. In the northern Sardinia Channel, westward flow is in agreement with earlier publications, but a coherent jet-like band attached to the shelf slope is missing. In the present case such band is apparently interrupted by the Sardinia anticyclone absorbing a significant fraction of the LIW coming from the Tyrrhenian. In the southern Sardinia Channel, previous findings are controversial. Perkins and Pistek (1990) and Garzoli and Maillard (1979) found westward flow, while Bouzinac et al. (1999) reported on eastward current direction. In a similar way, the flow west of the Channel is still under debate. There is no disagreement that the LIW confined to the southern slope of Sardinia turns anticyclonically around the island, but according to Ovchinnikov (1966) and models (cf. Wu and Haines, 1996) another vein separates from that LIW right off the southern tip of Sardinia and proceeds southwest to the Algerian coast. In the present observations, this vein is missing, but the northward flow along the Sardinian west coast is well reproduced. Probably, the variability of LIW flow at the western entrance of the Channel is caused by

sporadic advection of anticyclonic eddies of the Algerian Current (Millot, 1985).

In order to address the question of the origin of the low $S(S_{max})$ patch between Galite Bank and Skerki Bank, Fig. 12 displays the structure of potential temperature and salinity in different regimes of the survey area. For discrimination between different LIW regimes, the casts were separated in four classes according to location and $S(S_{max})$ (see Table 1). Fig. 12 reveals that above 250 dbar, Skerki LIW exhibits almost the same characteristics as Tyrrhenian LIW, whereas below 350 dbar, it is almost identical with Algerian LIW. That apparently had invaded the Skerki region from the west and later became detached by the southward migrating Tyrrhenian LIW in the Sardinia Channel. Below 350 dbar, the advection of Algerian LIW involved a freshening and cooling and simultaneously freshening and upward migration of the salinity maximum. The latter is visible from Fig. 9 (bottom) and the T/S diagram of Fig. 12. These findings agree with Sammari et al. (1999), who concluded that old LIW from the Algerian Basin proceeds east along the Tunisian slope up to the western exit of the Strait of Sicily, where it meets young LIW from the Eastern Mediterranean.

Table 1 *LIW regimes in the survey region. $S(S_{max})$ is the salinity of the LIW salinity maximum. The color coding refers to Fig. 12.*

LIW class	location	salinity range	color coding
Algerian	west of Sardinia Channel	$S(S_{max}) \leq 38.58$	blue
Skerki	between Galite Plateau and Skerki Bank	$S(S_{max}) \leq 38.60$	green
Strait of Sicily	Strait of Sicily	$38.74 \leq S(S_{max})$	red
Tyrrhenian	entire survey region	$38.66 \leq S(S_{max}) \leq 38.70$	orange

Fig. 12 reveals in addition important information on the LIW circulation in the Strait of Sicily. The T/S curves of seven out of ten CTD casts containing Strait-of-Sicily LIW are almost identical. The other three curves (marked by arrows), however, differ considerably; both temperature and salinity are lower and exhibit partly the characteristics of Tyrrhenian LIW and WIW (see above). As the corresponding CTD casts are all located on the Tunisian side of the Strait, it is concluded that a fraction of the Strait-of-Sicily LIW mixes with Tyrrhenian LIW and WIW in the Skerki Bank area, and recirculates cyclonically in the Strait. Evidence for such recirculation was already gained from Fig. 10.

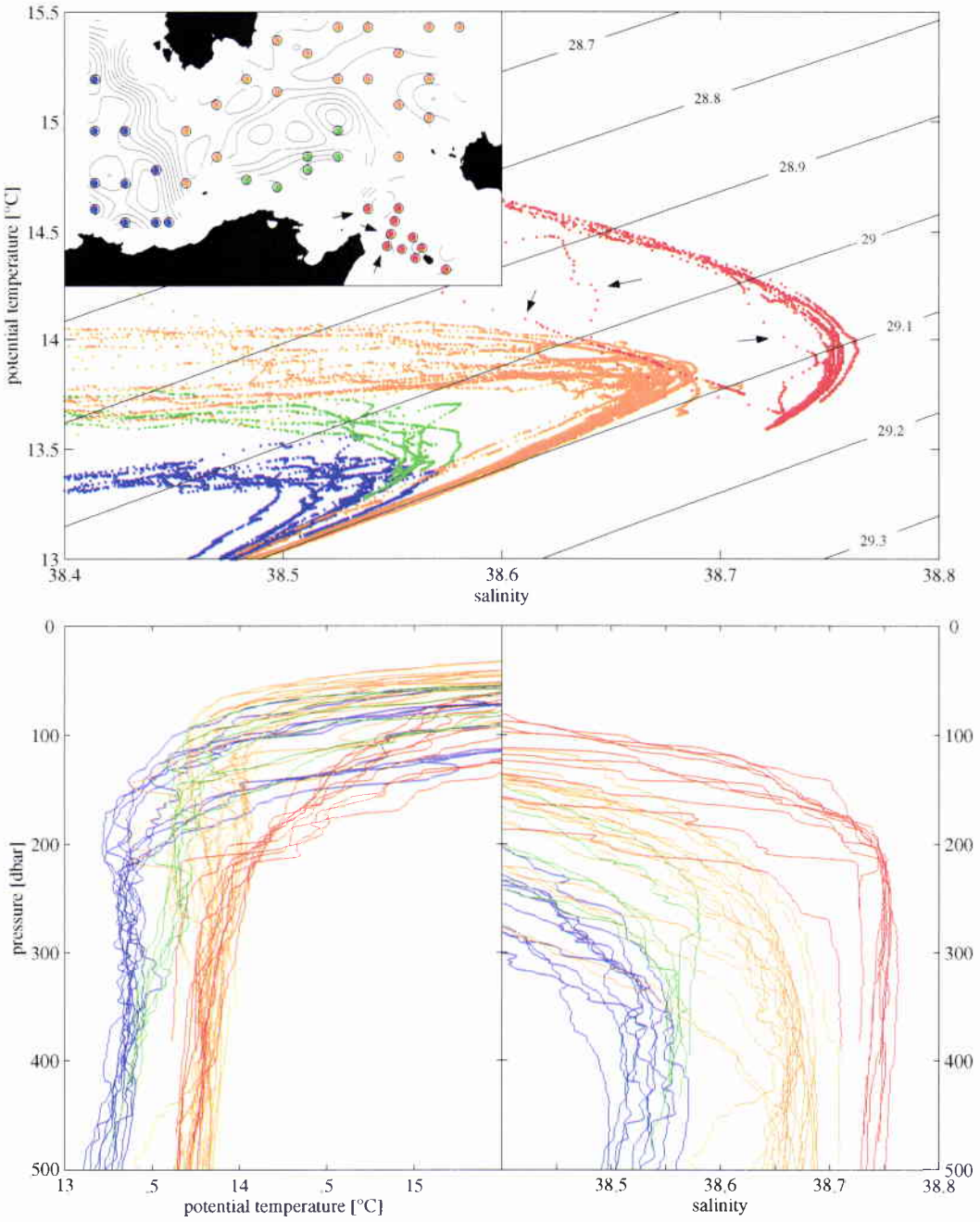

Figure 12 *Top: T/S diagram of the LIW range for different regimes of the survey area. Contours refer to potential density anomaly σ_0 [kg m^{-3}]. The color coding matches the color of the circles in the inset map indicating the positions of CTD stations. Contour lines in the inset map are identical to those in Fig. 9. Arrows in the T/S graph and in the inset map are marking those stations in the Strait of Sicily where LIW of Tyrrhenian origin was found. Bottom: Profiles of potential temperature [° C] (left) and salinity (right) of the top 500 dbar corresponding to the T/S graphs above.*

6

Sound velocity

The depth of the sound channel is characteristic for the sound velocity structure in the same way as the depth of the temperature and salinity extrema for the structure of the water masses. Sound velocity Sv was calculated from all CTD and XCTD casts, and the pressure of the sound velocity minimum $p(Sv_{min})$ (i.e. the depth of the sound channel) and the sound velocity at the minimum $Sv(Sv_{min})$ were objectively analysed and displayed in Fig. 13. The general tendency of the sound velocity structure is from low to high west–east. It is divided in two major regimes separated by a strong front running southwest–northeast from about Cape Bon to the western shelf of Sicily. Here, the sound velocity changes by about 2 m s^{-1} over a horizontal distance of less than 50 km. To the west of the front, sound velocity values are 1507–1509 m s^{-1} , while 1511–1513 m s^{-1} east of it. By contrast, the depth of the minimum exhibits a south–north trend controlled by two major fronts. The first is oriented northwest–southeast from west of Sardinia to about Skerki Bank, while the latter is aligned along the Algerian/Tunisian shelf break. Typical pressure changes across both fronts are about 50 dbar over 20 km. To the north of the northern front, the depth of the minimum exhibits little variability lying between 60 and 100 dbar. Another homogeneous region around 160 dbar is located between both fronts. The whole depth range is 60–280 dbar. The minima of less than 80 dbar are scattered at several locations to the north of the northern front, but the highest values exceeding 220 dbar are only found in the Strait of Sicily off Cape Bon.

Comparing the pressure fields of Fig. 13 and Fig. 7 reveals strinking similarities. As the same colorscale was applied to both figures, one can easily detect that the sound channel lies above the WIW core everywhere. The pressure difference is small where the WIW core is shallow and large where the WIW core is deep, e.g. east of Sardinia and off Algeria. A closer inspection of the data revealed that a shallow WIW core is correlated with large vertical temperature gradients while the temperature gradients are weak when the core is deep. Hence, the sound velocity is primarily temperature controlled and 'feels' the WIW temperature minimum where the WIW core is shallow; however, in those regions where the WIW core is deep, the change of sound velocity is controlled by pressure due to the small changes in temperature.

In order to make a statement about to what degree the situation found during our survey is representative, we have extracted the corresponding sound veloc-

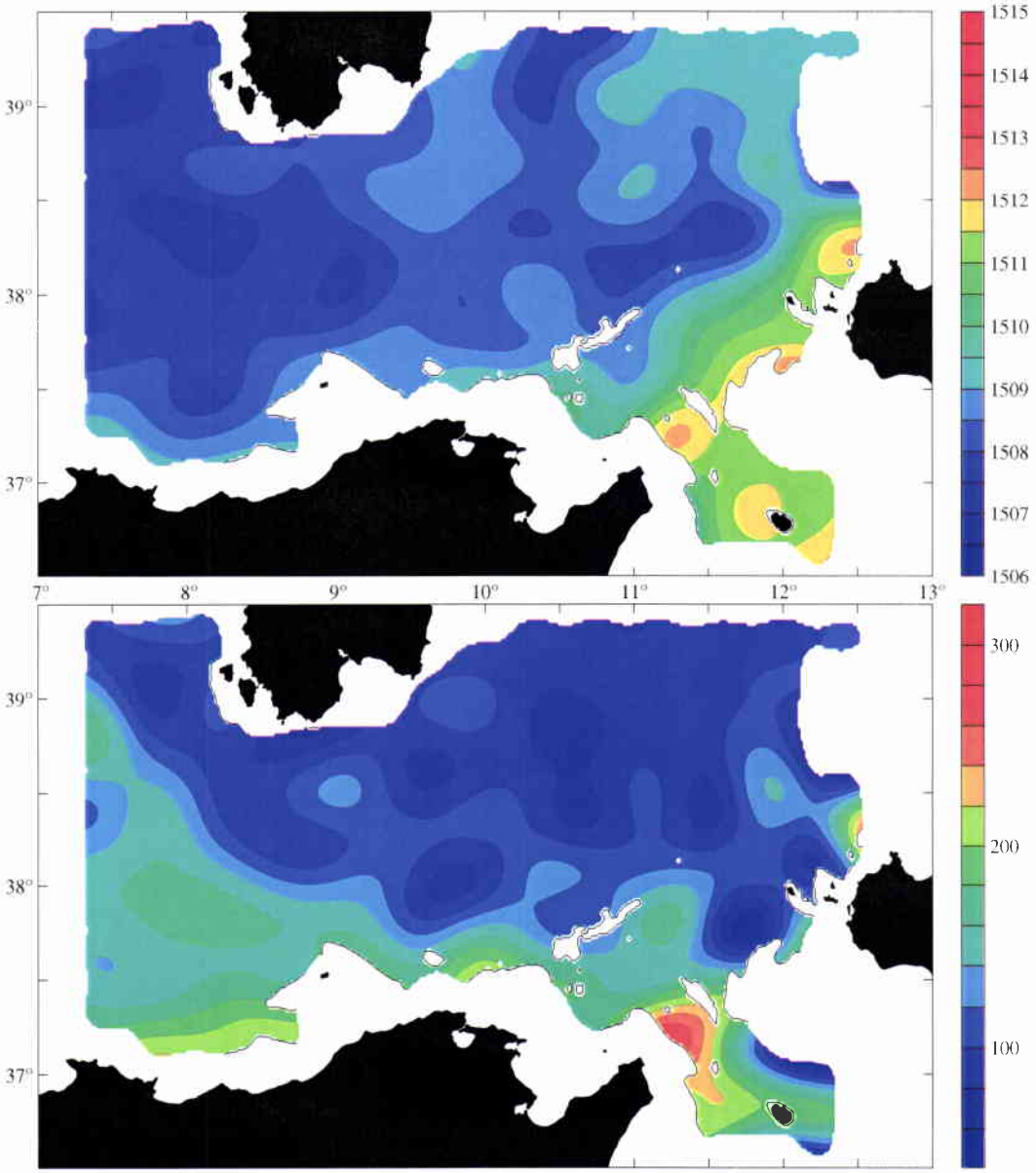

Figure 13 *Objectively analysed sound speed $Sv(Sv_{min})$ (top) and pressure $p(Sv_{min})$ [dbar] (bottom) of the sound velocity minimum. Black solid lines denote the intersection of the $p(Sv_{min})$ surface with the bathymetry H. Areas where the root mean square error of the analysed fields is greater than 2ϵ or $p(Sv_{min}) > H$ are left white.*

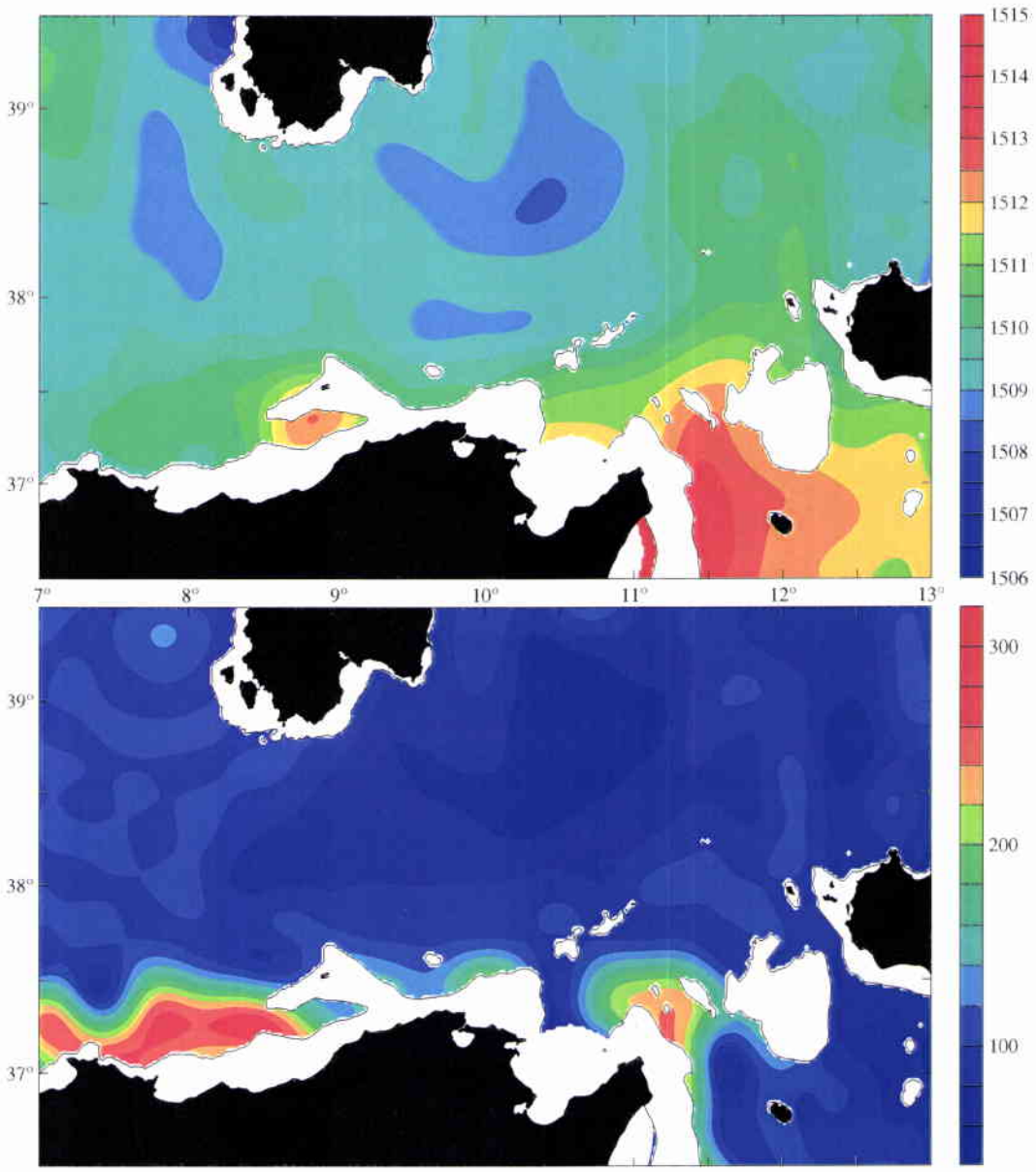

Figure 14 *Objectively analysed sound speed $Sv(Sv_{min})$ (top) and pressure $p(Sv_{min})$ [dbar] (bottom) of the sound velocity minimum from the GDEM October climatology. Black solid lines denote the intersection of the $p(Sv_{min})$ surface with the bathymetry H. Areas where the root mean square error of the analysed fields is greater than 2ϵ or $p(Sv_{min}) > H$ are left white.*

ity parameters from the GDEM October climatology (Generalized Digital Environmental Model, Naval Oceanographic Office, Stennis Space Center, Mississippi; http://www.navo.navy.mil/). According to Fig. 14, the sound velocity at the minimum is generally higher by about 1 m s^{-1} everywhere. The north–south contrasts are greater, but the gradients across the front between Cape Bon and Sicily are weaker. The northern part of that front is missing, instead a high sound velocity lobe is entending to the north towards the Tyrrhenian Sea. Significantly different is the depth of the sound channel. For convenience, Fig. 15 shows the difference between the channel depths obtained from GDEM and our survey, $p(Sv_{min}^{GDEM}) - p(Sv_{min}^{Oct96})$. In most parts of the survey area, the GDEM sound channel is shalllower by 20–60 dbar, in the Strait of Sicily the difference even reaches more than 170 dbar. Only at a few locations, e.g. southwest of Sardinia, along the Algerian shelf break and at the entrance to the Strait of Sicily, its depth is greater by up to 80 dbar.

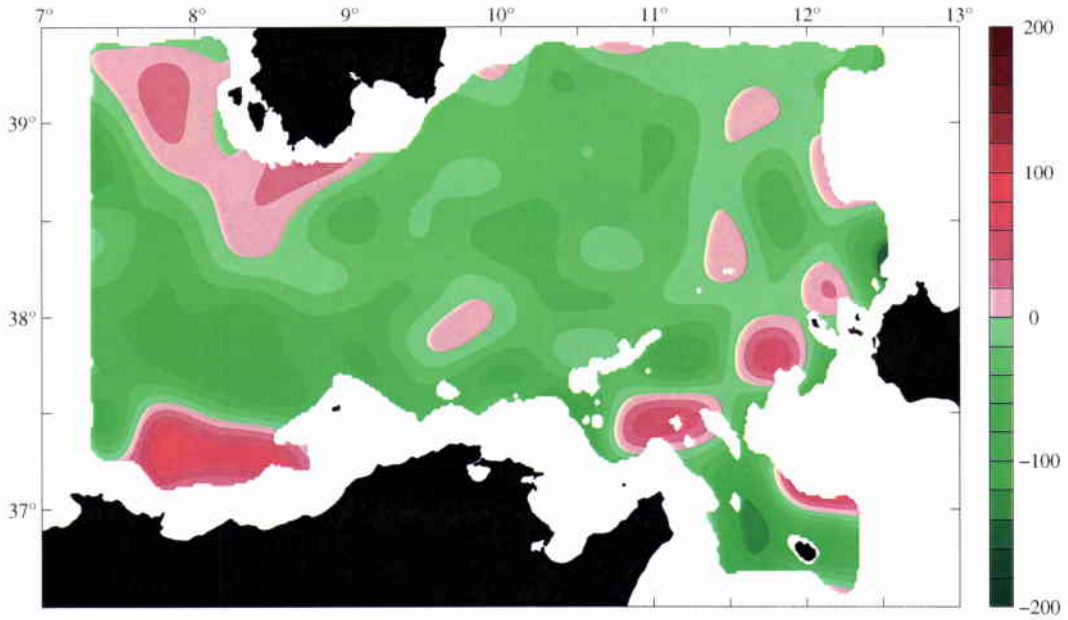

Figure 15 *Difference $p(Sv_{min}^{GDEM}) - p(Sv_{min}^{Oct96})$ of the sound channel depths obtained from GDEM climatology and our survey in October 1996. Units are [dbar]. Green coloring indicates that the GDEM sound channel is shallow, red means deeper. The contour interval is 20 dbar. For the depths of the sound channels cf. bottom panels of Figs. 14 and 13.*

7

Summary and conclusions

For the first time, a consistent pattern of the water mass distribution and circulation between the eastern Algerian Basin and the Strait of Sicily is obtained from a high resolution oceanographic survey in autumn 1996. The distribution of MAW (Modified Atlantic Water), WIW (Winter Intermediate Water) and LIW (Levantine Intermediate Water) were diagnosed by the core method and the velocity field was determined in terms of geostrophic currents and validated by direct measurements to large extent.

Between the Sardinia Channel and the Strait of Sicily, the large-scale flow of MAW and WIW is cyclonic. The cyclonic gyre is fed by eastward flow in the southern Sardinia Channel, and by some contribution coming from the northern Tyrrhenian Sea. MAW and WIW leave the cyclonic circulation via the Strait of Sicily. Outflow to the Tyrrhenian is accomplished northwest of Sicily and close to the Sardinian coast. The LIW pattern resembles that of the overlying MAW/WIW only north of a line between Sicily and Sardinia. In the Strait of Sicily the LIW flow is opposed. There is evidence that LIW from the Algerian Basin proceeds east along the Tunisian slope up to the western exit of the Strait of Sicily.

In the eastern Algerian Basin the flow of all water masses is to the east close to the Algerian shelf. Farther offshore, MAW flows mainly southwest contributing to additional inflow into Sardinia Channel, while the LIW is opposed to that supporting northward transport along the Sardinian shelf. No prevailing direction could be diagnosed for WIW.

In the Sardinia Channel, the MAW flow is mainly eastward. In the WIW range, eastward flow prevails only along the Algerian/Tunisian shelf, whereas the WIW in the northern half of the Channel goes west. The along Channel exchange of LIW appears to be confined to a narrow band of westward flow on the Sardinian shelf slope.

Mesoscale features were found to have an important impact on the general circulation. The most prominent examples are an intense anticyclone east of Sardinia preventing continuous flow from the Tyrrhenian Sea to the Algerian Basin at all levels, and another anticyclonic eddy between Sicily and Cape Bon supporting a secondary vein of MAW outflow into the Strait of Sicily close to the Sicilian coast.

Cyclonic motion in the Sardinia Channel is dragging parts of WIW and LIW from the Sardinian to the Tunisian coast. The circulation and water mass distribution is influenced by topographic obstacles, namely Galite Bank and Skerki Bank.

Except for a few locations, the depth of the sound channel lies deeper than that obtained from a climatological data base. This demonstrates the necessity of real-time measurements, because data bases do not take account of interannual variabilities.

All findings of this paper are based on the analysis of a single quasi-synoptic data set collected in October 1996. The described situation is only representative for this month of that particular year and it is not claimed that it represents any "mean" or "autumn" situation of this region. In order to find out to what extent the situation might represent mean conditions, it should be compared with climatological data sets. This may be subject of another study.

Acknowledgements

This work was performed at the SACLANT Undersea Research Centre in La Spezia, Italy. We would like to thank the crew of NRV *Alliance* and our technical staff for acquisition of the data. The ADCP data were processed by G. Baldasserini and A. Legner helped with the graphics. The satellite image was kindly provided by E. Nacini.

References

Astraldi, M., Gasparini, G.P., 1994. The seasonal characteristics of the circulation in the Tyrrhenian Sea, in: La Violette, P.E. (Ed.) *The Seasonal and Interannual Variability of the Western Mediterranean Sea*, Coastal and Estuarine Studies, **46**, Amer. Geophys. Union, 115–134.

Astraldi, M., Gasparini, G.P., Sparnocchia, S., Moretti, M., Sansone, E., 1996. The characteristics of the water masses and the water transport in the Sicily Strait at long time scales, *Bull. Inst. Océanogr., Monaco*, n°spécial **17**, 95–117.

Benzohra, M., Millot, C., 1995. Characteristics and circulation of the surface and intermediate water masses off Algeria, *Deep-Sea Res. I*, **42**, 10, 11803–11830.

Bethoux, J.-P., 1980. Mean water fluxes across sections in the Mediterranean Sea, evaluated on the basis of water and salt budgets and of observed salinities, *Oceanol. Acta*, **3**, 1, 79–88.

Bouzinac, C., Font, J., Millot, C., 1999. Hydrology and currents observed in the Channel of Sardinia during the PRIMO-1 experiment from November 1993 to October 1994, *J. Mar. Syst.*, **20**, 1–4, 333-355.

Carter, E.F., Robinson, A.R., 1987. Analysis models for the estimation of oceanic fields , *J. Atmosph. Ocean. Technol.*, **4**, 49–74.

Frassetto, R., 1972. A study of the turbulent flow and character of the water masses over the Sicilian Ridge in both summer and winter, *SACLANTCEN Conf. Proc.*, **7**, 38–44, SACLANT ASW Research Centre, La Spezia, Italy.

Garzoli, S., Maillard, C., 1979. Winter circulation in the Sicily and Sardinia Strait region, *Deep-Sea Res.*, **26**, A, 933–954.

Herbaut, C., Codron, F., Crépon, M., 1998. Separation of a coastal current at a Strait level: case of the Strait of Sicily, *J. Phys. Oceanogr.*, **28**, 7, 1346–1362.

Hopkins, T.S., 1988. Recent observations on the intermediate and deep water circulation in the Southern Tyrrhenian Sea, in: Minas, H.J., Nival, P. (Eds.) *Océanographie pélagique méditerraneénne*, *Oceanol. Acta*, special issue **N°9**, 41–50.

Katz, E.J., 1972. The Levantine Intermediate Water between the Strait of Sicily and the Strait of Gibraltar, *Deep-Sea Res.*, **19**, 507–520.

Krivosheya, V.G., 1983. Water circulation and structure in the Tyrrhenian Sea, *Oceanology*, **23**, 2, 166–171.

Krivosheya, V.G., Ovchinnikov, I.M., 1973. Peculiarities in the geostrophic circulation of the waters of the Tyrrhenian Sea, *Oceanology*, 13, 822-827.

Lacombe, H., Tchernia, P., 1960. Quelques traits généraux de l'hydrologie Méditerranéenne, *Cah. Océanogr.*, **12**, 8, 527–547.

Lacombe, H., Tchernia, P., 1972. Caractères hydrologiques et circulation des eaux en Méditerranée, in: Stanley, D.J. (Ed.) *The Mediterranean Sea*, Dowden Hutchinson and Ross, Stroudsbourg, Pennsylvania, 26-36.

Manzella, G.M.R., 1994. The seasonal variability of the water masses and transport through the Strait of Sicily. In: La Violette, P.E. (Ed.) *The Seasonal and Interannual Variability of the Western Mediterranean Sea*, Coastal and Estuarine Studies, **46**, Amer. Geophys. Union, 33–45.

Manzella, G.M.R., Gasparini, G.P., Astraldi, M., 1988. Water exchange between the eastern and western Mediterranean through the Strait of Sicily, *Deep-Sea Res.*, **35**, 6, 1021–1035.

Marullo, S., Santoleri, R., Bignami, F., 1994. The surface characteristics of the Tyrrhenian Sea: historical satellite data analysis, in: La Violette, P.E. (Ed.) *The Seasonal and Interannual Variability of the Western Mediterranean Sea*, Coastal and Estuarine Studies, **46**, Amer. Geophys. Union, 135–154.

Millot, C., 1985. Some features of the Algerian Current, *J. Geophys. Res.*, **90**, C4, 7169–7176.

Millot, C., 1999. Circulation in the Western Mediterranean Sea, *J. Mar. Syst.*, **20**, 1-4, 424–442.

Molcard, R., 1972. Preliminary results of current measurements in the Strait of Sicily in May 1970, *SACLANTCEN Conf. Proc.*, **7**, 82–95, SACLANT ASW Research Centre, La Spezia, Italy.

Ovchinnikov, I.M., 1966. Circulation in the surface and intermediate layers of the Mediterranean, *Oceanology*, **6**, 48–59.

Onken, R., Sellschopp, J., 1998. Seasonal variability of flow instabilities in the Strait of Sicily, *J. Geophys. Res.*, **103**, C11, 24799–24820.

Perkins, H., Pistek, P., 1990. Circulation in the Algerian Basin during June 1986, *J. Geophys. Res.*, **95**, C2, 1577–1585.

Pierini, S., Simioli, A., 1998. A wind-driven circulation model of the Tyrrhenian Sea area, *J. Mar. Syst.*, **18**, 161–178.

Robinson, A.R., Sellschopp, J., Warn-Varnas, A., Leslie, W.G., Lozano, C.J., Haley Jr., P.J., Anderson, L.A., Lermusiaux, P.F.J., 1999. The Atlantic Ionian Stream, *J. Mar. Syst.*, **20**, 1–4, 129–156.

Roussenov, V., Stanev, E., Artale, V., Pinardi, N., 1995. A seasonal model of the Mediterranean Sea general circulation. *J. Geophys. Res.*, **100**, C7, 13515–13538.

Salat, J., Font, J., 1987. Water mass structure near and offshore the Catalan coast during the winter of 1982 and 1983, *Ann. Geophys.*, **5B**, 1, 49–54.

Sammari, C., Millot, C., Taupier-Letage, I., Stefani, A., Brahmi, M., 1999. Hydrological characteristics in the Tunisia-Sardinia-Sicily area during spring 1995, *Deep-Sea Res. I*, **46**, 1, 1671–1703.

Shonting, D. H., Nacini, E., 1972. A summary of oceanographic data obtained in deep water in the Strait of Sicily in May 1970, *SACLANTCEN Conf. Proc.*, **7**, 45–67, SACLANT ASW Research Centre, La Spezia, Italy.

Sparnocchia, S., Gasparini, G.P., Astraldi, M., Borghini, M., Pistek, P., 1999. Dynamics and mixing of the Eastern Mediterranean outflow in the Tyrrhenian basin, *J. Mar. Syst.*, **20**, 1–4, 301–317.

Wu, P., Haines, K., 1996. Modeling the dispersal of Levantine Intermediate Water and its role in Mediterranean deep water formation, *J. Geophys. Res.*, **101**, C3, 6591–6607.

Wüst, G., 1961. On the vertical circulation of the Mediterranean Sea, *J. Geophys. Res.*, **66**, 10, 3261–3271.

Zavatarelli, M., Mellor, G.L., 1995. A numerical study of the Mediterranean Sea circulation, *J. Phys. Oceanogr.*, **25**, 6, Part II, 1384–1414.

Report no. changed (Mar 2006): SM-329-UU

Document Data Sheet

Security Classification		Project No.
UNCLASSIFIED		01-A
Document Serial No.	**Date of Issue**	**Total Pages**
SM-329	December 2001	40 pp.

Author(s)

Onken, R., Sellschopp, J.

Title

Water masses, sound velocity structure and circulation between the eastern Algerian Basin and the Strait of Sicily in October 1996.

Abstract

The investigation is based on data collected between the eastern Algerian Basin and the Strait of Sicily and in the southern Tyrrhenian Sea. The major pathways of water masses are identified by the core method and geostrophic currents are derived from the objectively analyzed density field

Between the Sardinia Channel and the Strait of Sicily, the large-scale circulation of Modified Atlantic Water (MAW) and Winter Intermediate Water (MIW) is found to be cyclonic. Inflow into the gyre occurs via the Sardinia Channel by means of a boundary current attached to the Algerian coast and from the northern Tyrrhenian. The outflow is accomplished via the Strait of Sicily and to the Tyrrhenian. The Levantine Intermediate Water (LIW) flow resembles that of MAW/MIW in the southern Tyrrhenian, but is opposed in the Strait of Sicily and off Tunisia. Outflow to the Algerian Basin occurs south of Sardinia. In the eastern Algerian Basin the flow direction of all water masses is eastward close to the Algerian shelf. Farther offshore, MAW flows mainly southwest whereas the LIW is opposed to that supporting northward transport along the Sardinian shelf. The large-scale flow of all water masses is perturbed by mesoscale eddies. The impact of topographic obstacles is investigated.

Keywords

Mediterranean - Modified Atlantic Water - Winter Intermediate Water – Levantine Intermediate Water

Issuing Organization

North Atlantic Treaty Organization
SACLANT Undersea Research Centre
Viale San Bartolomeo 400, 19138 La Spezia, Italy

[From N. America: SACLANTCEN (New York) APO AE 09613]

Tel: +39 0187 527 361
Fax:+39 0187 527 700

E-mail: library@saclantc.nato.int

Report no. changed (Mar 2006): SM-329-UU

The SACLANT Undersea Research Centre provides the Supreme Allied Commander Atlantic (SACLANT) with scientific and technical assistance under the terms of its NATO charter, which entered into force on 1 February 1963. Without prejudice to this main task - and under the policy direction of SACLANT - the Centre also renders scientific and technical assistance to the individual NATO nations.

SACLANT Undersea Research Centre
Viale San Bartolomeo 400
19138 San Bartolomeo (SP), Italy

tel: +39 0187 527 (1) or extension
fax: +39 0187 527 700

e-mail: library@saclantc.nato.int

NORTH ATLANTIC TREATY ORGANIZATION